COMPARISON OF HARD SCATTERING MODELS FOR PARTICLE PRODUCTION AT LARGE TRANSVERSE MOMENTA. II. TRANSVERSE MOMENTUM AND RAPIDITY DEPENDENCE OF π^+ AND π^- SINGLE PARTICLE DISTRIBUTIONS

By A. Schiller, E.-M. Ilgenfritz, J. Kripfganz*, H.-J. Möhring, Gisela Ranft and J. Ranft

Sektion Physik, Karl-Marx-Universität, Leipzig**

(Received June 16, 1977; final version received August 16, 1977)

Single particle distributions of π^+ and π^- at large $p_\perp$ are analysed using various hard collision models: $qq \to qq$, $q\bar{q} \to M\bar{M}$, $qM \to qM$. The $p_\perp$ dependence at $\theta_{cm} = 90°$ is well described in all models except $q\bar{q} \to M\bar{M}$. This model has problems with the ratios $(pp \to \pi^+ + X)/(pp \to \pi^- + X)$ at large $x_\perp$ and with $(pp \to \pi^0 + X)/(\pi^\pm p \to \pi^0 + X)$. Presently available data on rapidity distributions of pions in π^-p and $p\bar{p}$ collisions are at rather low $p_\perp$ (however large $x_\perp = 2p_\perp/\sqrt{s}$) where it is not obvious that hard collision models should dominate. The data, in particular the π^-/π^+ asymmetry, are well described by all models except $qM \to Mq$ (CIM). At large values of $p_\perp$ significant differences between the models are predicted.

1. Introduction

In a previous paper [1] (henceforth denoted by I) we compared four different hard collision models with the data on opposite side rapidity correlations and found that the data strongly constrain the cross section of the irreducible hard subcollision $d\sigma/d\hat{t}$. In the present paper we study again these four models, (*i*) $qq \to qq$, (*ii*) $\bar{q}q \to \bar{M}M$, (*iii*) $qM \to Mq$ (CIM), and (*iv*) $qM \to qM$ (gluon exchange) with phenomenological hard collision cross sections as determined in I. We analyse data on single particle distributions and π^-/π^+ ratios as function of the transverse momentum [2–5] at $\theta_{cm} = 90°$ and as function of the rapidity [6–8]. As in I we restrict ourselves to the production of pions.

In Section 2 we describe the calculation of single particle distributions in the hard scattering models studied. In Section 3 we consider the transverse momentum dependence of single particle distributions at $\theta_{cm} = 90°$. The result of a least square fit of the four

* Presently at CERN, Geneva, Switzerland.

** Address: Sektion Physik, Karl-Marx-Universität, Karl-Marx-Platz, 701 Leipzig, DDR.

models to data is described in Section 3 and we discuss in detail the π^+/π^- ratio as function of $p_\perp$ and the ratio $R(p/\pi)$ of π^0 production in pp and πp collisions. In Section 4 we discuss the rapidity dependence of single particle distributions and π^-/π^+ ratios in π^-p and $\bar{p}p$ collisions. The models are compared with data with $p_\perp > 1$ GeV/c [6–8] as presently available and we discuss differences predicted by the models at higher $p_\perp$. In Section 4 we summarize our results and compare the successes and failures of the four models studied.

2. *Single particle distributions in hard scattering models*

Inclusive single particle distributions in hard scattering models are given by the following expressions [9, 10],

$$E_C \frac{d^3\sigma}{d^3p_C} = \frac{4}{\pi x_{\perp C}^2} \sum_{\substack{i,j \\ k,l}} \iint dx_1 dx_2 F_A^i(x_1) F_B^j(x_2) \frac{\eta}{(1+\eta)^2} \frac{d\sigma}{d\hat{t}} G_C^k(z). \tag{2.1}$$

We use the fragmentation functions $F_H^i(x)$ and $G_H^k(z)$ in the form discussed in detail in paper I. For the hard collision cross section we use the best parametrizations found in I and [11]. The leading term for this parametrization corresponds to

$$\frac{d\sigma}{d\hat{t}} = c^i \frac{1}{\hat{s}^{(n-3)}\hat{t}^3}; \quad n \approx 4. \tag{2.2}$$

c^i normalizes the cross section. The detailed structure of Eq. (2.1) depends on the particular hard scattering model considered.

3. *Dependence on transverse momentum at* $\theta_{cm} = 90°$

3.1. Least square fit of the four models to data

In order to compare the four models to data, to optimize the parameters and to compare the models among themselves we have performed a least square fit. For the fit we use the following data:

(*i*) production cross sections for $pp \to \pi^+$ and $pp \to \pi^-$ at $\sqrt{s} = 19.4$, 23.8 and 27.4 GeV and $p_\perp > 3$ GeV/c from the Chicago–Princeton collaboration [2] and at $\sqrt{s} = 53$ GeV and $p_\perp > 2$ GeV/c from the British–Scandinavian collaboration [4],

(*ii*) π^0 production cross sections for $pp \to \pi^0$ at $\sqrt{s} = 52.7$ GeV and $p_\perp > 2.5$ GeV/c from the CERN–Columbia–Rockefeller collaboration [3],

(*iii*) ratios $R\left(\frac{p}{\pi}\right) = E\frac{d^3\sigma}{d^3p}\Big|_{pp\to\pi^0X} \Big/ E\frac{d^3\sigma}{d^3p}\Big|_{\pi^\pm p\to\pi^0X}$ at $\sqrt{s} = 13.7$ and 19.4 GeV and $p_\perp > 1.5$ GeV/c from the BNL-Caltech-LBL collaboration [5].

In the least square fit of the four models we obtain the following results.

(*i*) $qq \to qq$

First fit:

We use the quark distribution function according to the fit of Barger and Phillips [12] and the other distributions described in I. In the fit we have the following free parameters: the normalization c^i and the power n in the hard scattering cross section (2.2). Furthermore, to allow for different absolute normalization in different experiments we use free normalization parameters $c^i_{\pi^0}$ for the π^0 distribution and $c(p/\pi)$ for the ratio $R(p/\pi)$. The parameters obtained in the fit are given in the first line of the Table I. A good fit to the data is achieved

TABLE I

Least squares fit

Model	c^i [mbGeV$^{2(n-1)}$]	n	$c^i_{\pi^0}$	$c\left(\frac{p}{\pi}\right)$	F^{π}_{0u}	α_{nf}	χ^2/degree of freedom
(*i*)							
qq → qq (1)	1.38×10^4	4.72	5.20	2.19	—	—	7.8
qq → qq (2)	1.38×10^4	4.72	5.19	—	0.16	—	7.7
(*ii*)							
$q\bar{q}$ → $M\bar{M}$	1.14×10^5	4.51	2.56	4.76	—	0.0037	14.3
(*iii*)							
qM → Mq CIM	2.52×10^3	4.32	2.20	3.16	—	0.0068	3.7
(*iv*)							
qM → qM (gluon exchange)	4.94×10^3	4.45	2.51	2.44	—	0.011	6.14

inspite of the large χ^2 value. This large χ^2 value results from using only statistical errors (about 5%) and not the larger systematic and normalization error of the data [2]. The power $n = 4.72$ is somewhat larger than $n = 4.1$ determined in [2]. The reason could be that we use only data points with $p_\perp > 3$ GeV/c and that we use in addition the data at $\sqrt{s} = 53$ GeV (Ref. [4]). The parameter $c(p/\pi) = 2.19$ indicates that the ratio $R(p/\pi)$ according to the model is only half as large as the data. What are the possibilities to increase this ratio in the model?

The quark distribution functions are determined from deep inelastic data and should not be changed. The quark distribution functions in pions

$$F^{\pi^+}_{\text{valence}} = 2x(1-x) \tag{3.1}$$

are determined using dimensional counting arguments [14] and could be wrong. The hard collision cross sections and the quark fragmentation functions are the same in both reactions in pp → π^0X and πp → π^0X. First we have tried to obtain $c(p/\pi) = 1$ by decreasing the sea contribution to the pion fragmentation function F^{π}_{q}. No acceptable fit was obtained.

Second fit:

Next we changed $F^{\pi}_{\text{valence}}(x)$ into

$$F^{\pi}_{\text{valence}}(x) = F^{\pi^+}_{0u} = \text{const.} \tag{3.2}$$

for $x > x_0 > 0$ similarly as the $F^{\pi}_{q}(x)$ functions of Field and Feynman [13]. A good fit was obtained with $F^{\pi}_{0} = 0.16$. All parameters for this fit are given in the 2nd line of Table I. We conclude: The hard scattering model with the phenomenological qq → qq scattering cross section describes single particle distributions at $\theta_{\text{cm}} = 90°$ rather well. However, the ratios $R(\text{p}/\pi)$ as measured can only be obtained with a flattish valence quark distribution in pions as introduced by Field and Feynman [13].

(*ii*) $q\bar{q} \to M\overline{M}$:

The better fit was obtained using the quark distribution function of McElhaney and Tuan [15]. The free parameters are the same as in the first fit using the model qq → qq, c^i, n, $c^i_{\pi^0}$, $c(\text{p}/\pi)$ and in addition the fraction of nonfragmenting meson secondaries α_{nf}

$$E\frac{d^3\sigma}{d^3p} = (1-\alpha_{\text{nf}})E\frac{d^3\sigma}{d^3p}\bigg|_{\text{f}} + \alpha_{\text{nf}}E\frac{d^3\sigma}{d^3p}\bigg|_{\text{nf}}. \tag{3.3}$$

The best parameters obtained are given in Table I. The χ^2 is rather bad; The large value of $c(\text{p}/\pi)$ indicates that $R(\text{p}/\pi)$ is difficult to fit in this model. The shape of $R(\text{p}/\pi)$ agrees with the data but the disagreement in normalization $c(\text{p}/\pi)$ is too large. A similar but somewhat smaller disagreement was obtained already by Combridge [16]. We conclude: The model describes single particle distributions at large $x_\perp$ values rather badly.

(*iii*) qM → Mq (CIM) [17]

The free parameters in the fit are as above c^i, n, $c^i_{\pi^0}$, $c(\text{p}/\pi)$ and α_{nf}. The results of the fit are given in the Table I. The χ^2 value is the best of all fits reported here. The ratio $R(\text{p}/\pi)$ according to the model disagrees by the factor $c(\text{p}/\pi) = 3.16$ with the data. The normalization of the $F(x)$ functions is not strongly constrained by sum rules. Therefore it seems that the model is flexible enough to obtain $c(\text{p}/\pi) = 1$ with a suitable modification of these fragmentation functions. We conclude: Single pion production at $\theta_{\text{cm}} = 90°$ might be well described in the hard scattering model with the qM → Mq mechanism (CIM). This model uses however a phenomenologically determined hard scattering cross section with a $f(\eta)$ function as determined in paper I $\left(\text{leading behaviour } \frac{d\sigma}{d\hat{t}} \sim \frac{1}{\hat{s}\hat{t}^3}\right)$.

(*iv*) qM → qM (gluon exchange):

The parameters are the same as for model (*iii*). The result of the fit is given in Table I. The fit is worse then the one of model (*iii*). The fraction of non-fragmenting meson constituents α_{nf} as determined for models (*ii*), (*iii*) and (*iv*) is in the same order of magnitude as determined by Ellis, Jacob and Landshoff [19] from an analysis of opposite side correlations.

3.2.The ratio π^+/π^- in pp and pn collisions

We find: The model (*i*) qq → qq leads to good agreement for $x_\perp > 0.3$, but seems to give a somewhat too large π^+/π^- for $0.1 < x_\perp < 0.3$. The model (*ii*) $q\bar{q} \rightarrow M\bar{M}$ agrees rather well for $x_\perp < 0.3$ but is too small for larger $x_\perp$ values. The model (*iii*) qM → Mq (CIM) agrees rather well at all $x_\perp$ values. This good fit is obtained by the additional freedom in the model as compared with model (*i*). At low $p_\perp$ values the term — where the mesons

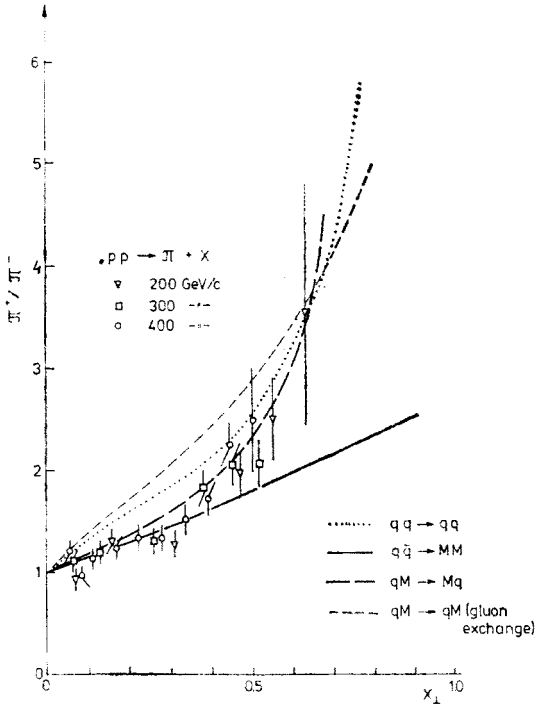

Fig. 1. The π^+/π^- ratio versus $x_\perp$ for pp collisions at 200, 300 and 400 GeV/*c*. The data is from Ref. [2]. It is compared with the four models as described in the text

and quarks fragment — dominates. At large $p_\perp$ values the term with non-fragmenting mesons dominates. The model (*iv*) qM → qM (gluon exchange) agrees only at large $x_\perp$ values; at small $x_\perp$ values it gives too large a π^+/π^- ratio. The π^+/π^- ratios favour either the CIM or a model where $q\bar{q} \rightarrow M\bar{M}$ dominates at low $x_\perp$ and qq → qq at large $x_\perp$. The experimental data for π^+/π^- in p+"n" collisions at $\theta_{cm} = 90°$ according to Ref. [2] are consistent with $\pi^+/\pi^- = 1$ for all $x_\perp$. All models considered are constructed consistent with this observation.

3.3. π^0 production in pp and πp collisions

In Figure 2 we compare the ratio $R(p/\pi)$ as function of $x_\perp$ according to the four models with the parameters obtained in the fit, see Table I.

We find: The model (*i*) qq → qq (2^{nd} fit) agrees in the total $x_\perp$ range very well with the data. The model (*ii*) $q\bar{q} \rightarrow M\bar{M}$ agrees in shape but the difference in normalization

cannot be understood, as discussed already above. The model (*iii*) qM → Mq (CIM) agrees in shape for $x_\perp > 0.2$. There is enough freedom in the model to remove the difference in normalization. The rise of the model prediction for $x_\perp$ below 0.2 might indicate that this model does not dominate at small $x_\perp$ values. Model (*iv*) behaves similar as model (*iii*), agrees however somewhat better at small $x_\perp$.

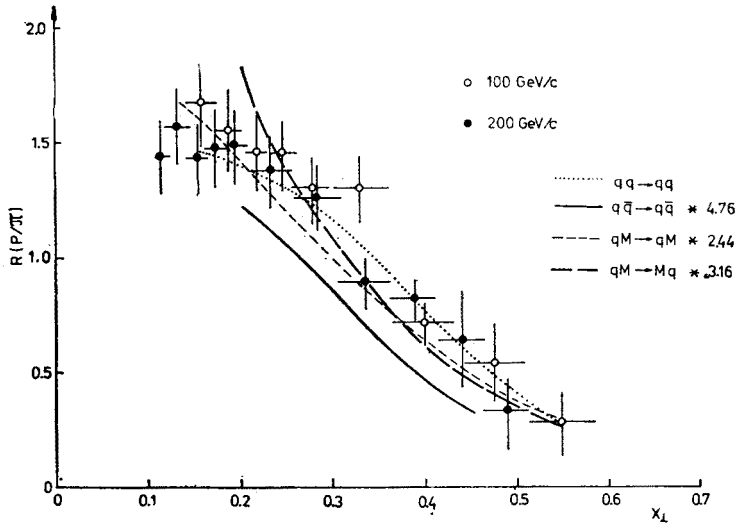

Fig. 2. The ratio of the invariant cross sections versus $x_\perp$ for $pp \to \pi^0 X$ and $\pi^- p \to \pi^0 X$ at 100 and 200 GeV/c. The data is from Ref. [5]. It is compared with the four models described in the text

4. The y dependence of single particle distributions

In this section we use the models with the hard scattering cross sections as determined in paper I and parameters as found by the fit to single particle distributions at $\theta_{cm} = 90°$ and calculate the rapidity dependence of single particle distributions. Only a rather limited amount of data on rapidity dependence of single particle distributions at large transverse momentum is available from counter experiments at the ISR [4,20] and Fermi-Lab [21]. Recently data on π^+ and π^- production at $p_\perp > 1$ GeV/c became available from bubble chamber experiments $\pi^- p \to \pi^+ \pi^- X$ at $\sqrt{s} = 5.6$ and 13.7 GeV [7] and 19.4 GeV [6] and $\bar{p}p \to \pi^+ \pi^- X$ at $\sqrt{s} = 5.6$ GeV [8]. The transverse momenta of these data are rather low, certainly at the limit where the hard scattering mechanism takes over from the low $p_\perp$ component. The data show however a strong rise of the π^+/π^- asymmetry with increasing transverse momentum. π^+/π^- asymmetry for the data observed at $p_\perp > 1$ GeV/c is significantly larger than found at low $p_\perp$. We note also that due to the low collision energy in these experiments the $x_\perp$ is rather high ($0.1 \lesssim x_\perp \lesssim 0.4$). Therefore we try to understand this asymmetry as resulting from the hard scattering mechanism. The data of Fretter et al. [6] were already analysed in such a way within the quark fusion model by Combridge [16].

We note also that the π^+ and π^- rapidity distributions according to hard scattering models change rather smoothly with increasing transverse momentum and show at

$p_\perp = 1$ GeV/c already all characteristic features. In Fig. 3 we plot the π^+ and π^- rapidity distribution in $\pi^-p \to \pi^+\pi^- + X$ at $\sqrt{s} = 20$ GeV in the qq → qq model. For $p_\perp = 1.0$, 2.5 and 5.5 GeV/c with rising transverse momentum both rapidity distributions become more narrow and the asymmetry rises.

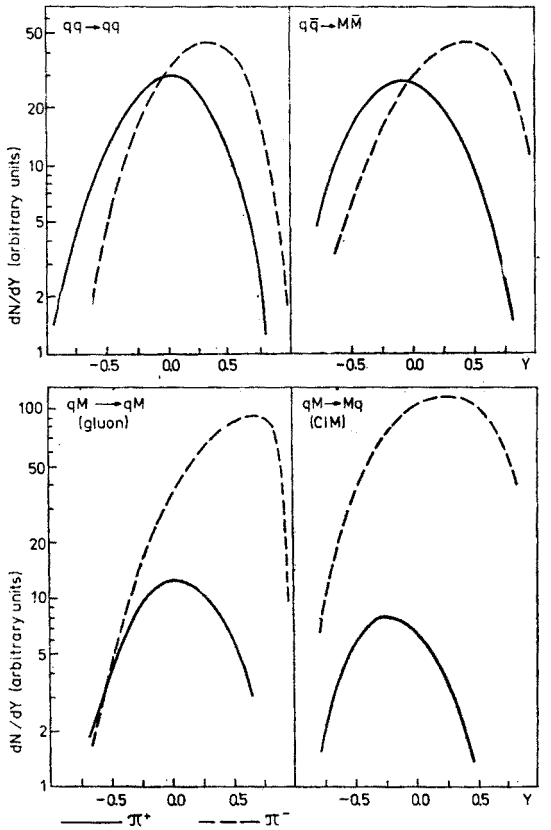

Fig. 3. Theoretical rapidity distributions obtained with the hard scattering subprocess qq → qq for the reactions $\pi^-p \to \pi^+X$ and $\pi^-p \to \pi^-X$ at $\sqrt{s} = 20$ GeV and at transverse momenta $p_\perp = 1$, 2.5, 4 and 5.5 GeV/c

In Figures 4 and 5 we compare the π^+ and π^- distributions in π^-p collisions with hard scattering models, in Fig. 6 we compare with data on $p\bar{p}$ collisions. In part a) of the Figures we compare the experimental data on π^+ and π^- rapidity distributions for $p_\perp > 1$ GeV/c with two of the hard collision models. In the part b) of the three Figures we plot the data in the form of the ratio

$$\frac{\pi^-}{\pi^+} = \frac{E\dfrac{d^3\sigma}{d^3p}\Big|_{\pi^-p\to\pi^-X}}{E\dfrac{d^3\sigma}{d^3p}\Big|_{\pi^-p\to\pi^+X}} \tag{4.1}$$

as function of rapidity and compare with the ratios calculated in all four models considered. In the hard scattering models (*ii*) to (*iv*) where meson constituents participate the plotted curves correspond to the superposition of fragmenting and non-fragmenting mesons as

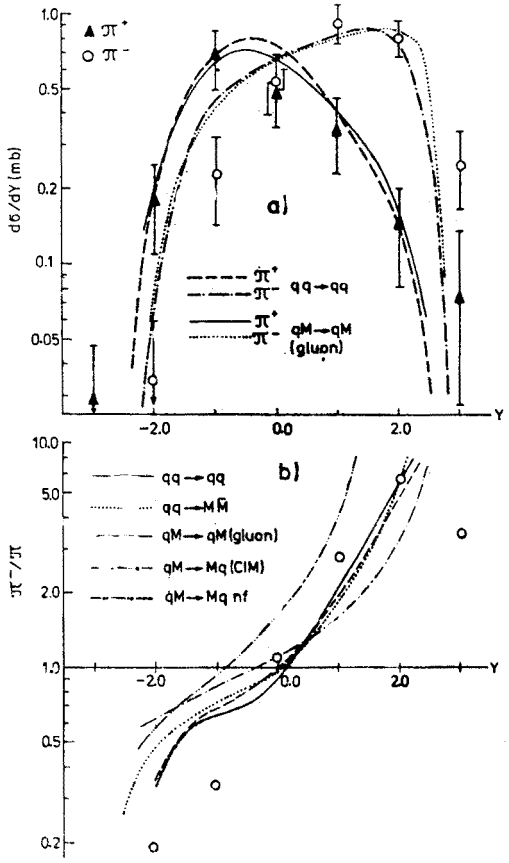

Fig. 4

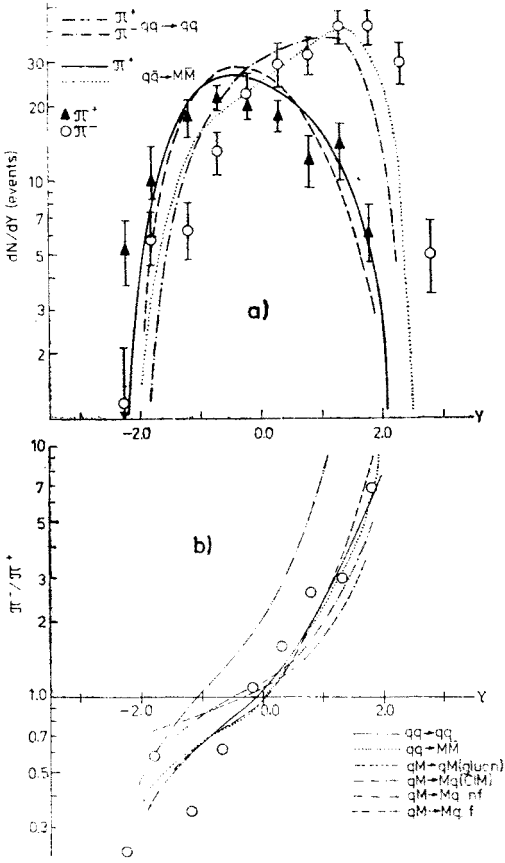

Fig. 5

Fig. 4. Comparison of π^+ and π^- rapidity distributions in π^-p collisions at $\sqrt{s} = 13.7$ GeV [7] for $p_\perp > 1$ GeV/c with hard collision models: a) comparison of the data with the rapidity distributions according to the models qq → qq and $q\bar{q} \to M\bar{M}$, b) comparison of the ratio π^-/π^+ with the ratios calculated according to the four models studied

Fig. 5. Comparison of π^+ and π^- rapidity distributions in π^-p collisions at $\sqrt{s} = 19.4$ GeV [6] for $p_\perp > 1$ GeV/c with hard collision models: a) comparison of the data with the rapidity distributions according to the models qq → qq and qM → qM (gluon exchange), b) comparison of the ratio π^+/π^- with the ratios calculated according to the four models studied

discussed in Section 3. The contribution with fragmenting and non-fragmenting mesons in the qM → Mq model differ strongly from each other. Therefore, when plotting the ratios π^-/π^+ we plot also these two contributions separately. As discussed already in Section 3 the term with non-fragmenting mesons dominates at large $p_\perp$; at small $p_\perp$ for the data in Figures 3 to 6 the component with fragmenting mesons dominates in the central

region. We remind the reader also that all available data on same side correlations demand an appreciable contribution from fragmenting mesons [19], [22].

Comparing the models with the data we find: The qq → qq model agrees well with the data of all experiments. The π^-/π^+ asymmetry is somewhat smaller than in the data, an effect which is due to our neglecting transverse momenta in the jet fragmentation.

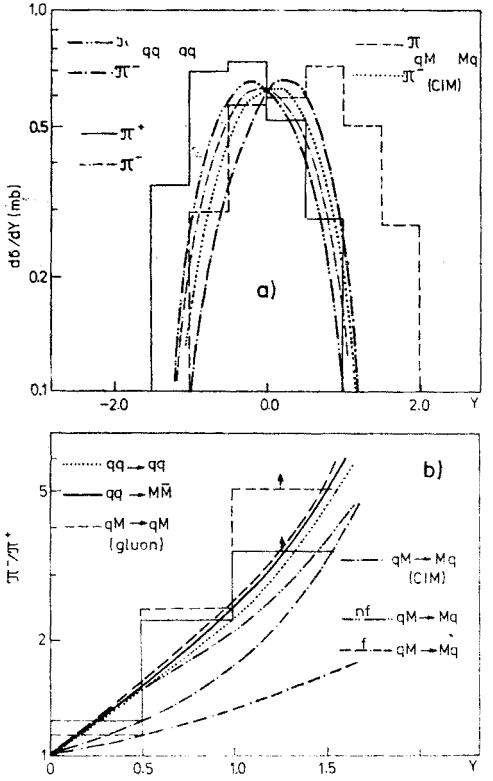

Fig. 6. Comparison of π^+ and π^- rapidity distributions in $\bar{p}p$ collisions at $\sqrt{s} = 6.6$ GeV [8] for $p_\perp >$ GeV/c with hard collision models: a) comparison of the data with the rapidity distributions according to the models qq → qq and qM → Mq (CIM), b) comparison of the ratio π^-/π^+ with the ratios calculated according to the four models studied

Calculated rapidity distributions become wider if the transverse momentum in the jet decay is taken into account, e. g. using the methods described in Ref. [23].

The prediction of the $q\bar{q} \to M\bar{M}$ and qM → qM (gluon exchange) models at $p_\perp = 1$ GeV/c are nearly the same as those from the qq → qq model. The π^-/π^+ asymmetry according to the qM → Mq (CIM) model are smaller than in the data and in the other three models. This is due to the dominance of the fragmenting contribution at the given $p_\perp = 1$ GeV/c. The rapidity distributions calculated depend only weakly on the details of the parton distribution function $F_A^i(x)$. In the quark-fusion model where this influence is strongest no significantly different behaviour is found using the distribution function due to Barger and Phillips [12] or McElhaney and Tuan [15].

To study the differences of the model predictions at larger $p_\perp$ we plot in Figure 7 the rapidity distributions of π^+ and π^- in π^-p collisions at $\sqrt{s} = 20$ GeV and $p_\perp = 5.5$ GeV/c. In the models with meson constituents non-fragmenting mesons dominate at this large $p_\perp$.

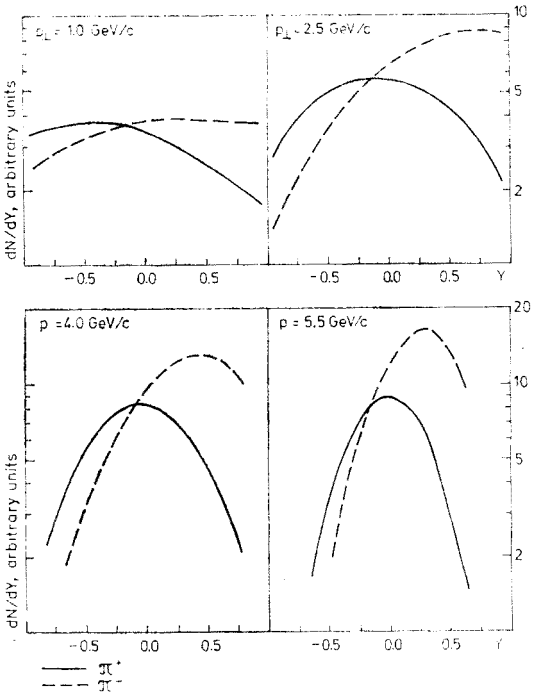

Fig. 7. Rapidity distributions of π^+ and π^- in $\pi^-p \to \pi^+X$ and $\pi^-p \to \pi^-X$ collisions at $\sqrt{s} = 20$ GeV and $p_\perp = 5.5$ GeV/c from hard collision models

We find strong differences in the behaviour of the qq → qq and $q\bar{q}$ → MM models on the one hand and the qM → qM and qM → Mq models on the other hand. In the latter two models, π^- production dominates also in backward direction.

5. *Summary and conclusions*

In Table II we collect the conclusions and problems found in the comparison of hard scattering models with data. The conclusions regarding single particle distributions result from the studies in the present paper; opposite side rapidity correlations were studied in I. In addition we collect conclusions from same side correlations and other comparisons with experiment taken from Refs [1–3, 22–35] of paper I.

All models explain some features of the data and there are some problems in all of the models. It seems to be unlikely that any one of the models studied alone would eventually account for all the data. As found in I the hard scattering cross sections $d\sigma/d\hat{t}$ are strongly constrained by opposite side correlations and some originally proposed cross

TABLE II

Conclusions from the comparison of hard scattering models with data (abbreviations: f = contribution with fragmenting meson, nf = contribution with non-fragmenting meson)

	$qq \to qq$	$q\bar{q} \to M\bar{M}$	$qM \to qM$ (CIM)	$qM \to qM$
Single particle distributions — $p_\perp$ dependence in pp	ok	Problems with π^+/π^-	ok, superposition of f and nf mesons needed for π^+/π^- ratio	ok
— beam ratio $R(p/\pi)$	ok, but flat $F^{\pi}_{q\ \text{valence}}(x)$ needed	problems with absolute value	ok	ok
— y distribution in πp and $\bar{p}p$ at $p_\perp = 1$ GeV/c	ok	ok	π^-/π^+ asymmetry too small	ok
Opposite side correlations — y dependence, shape	ok quark form factors excluded	ok trigger from f prefered	ok trigger from nf preferred, $\frac{d\sigma}{d\hat{t}} \sim \frac{1}{\hat{s}^2\hat{u}^2} + \frac{1}{\hat{s}^4}$ excluded	ok trigger from f preferred
— $\frac{d\sigma}{dx_e}$ and normalization of y dependence	problems with absolute normalization in all models proposed corrections: deviations from scaling of $G(z)$, superposition of f and nf, transverse momenta of partons in hadrons and of hadrons in jets			
Same side correlations and same side associated multiplicities	ok	Only if contribution from f mesons present at trigger side		

sections are excluded. The model most seriously in trouble with data seems to be $q\bar{q} \to M\bar{M}$. As found in the present paper rapidity distributions and in particular π^-/π^+ asymmetries in π^-p reactions measured at larger transverse momenta seem to provide further possibilities to exclude some of the models.

REFERENCES

[1] E.-M. Ilgenfritz, J. Kripfganz, H.-J. Möhring, G. Ranft, J. Ranft, A. Schiller, *Acta Phys. Pol.* **B9**, 15 (1978), henceforth denoted by I.

[2] D. Antreasyan et al., *Phys. Rev. Lett.* **38**, 112 (1977).

[3] F. W. Büsser et al., *Phys. Lett.* **46B**, 471 (1973).

[4] B. Alper et al., *Nucl. Phys.* **B100**, 237 (1975).
[5] G. Donaldson et al., *Phys. Rev. Lett.* **36**, 1110 (1976).
[6] W. B. Fretter et al., *Phys. Lett.* **57**, 197 (1975).
[7] J. Bartke et al., *Nucl. Phys.* **B117**, 293 (1976).
[8] E. G. Boos et al., Alma-Ata–Dubna–Moscow–Kosice–Prague–Helsinki collaboration, paper 903 submitted to the 18-th International Conference on High Energy Physics, Tbilisi 1976.
[9] S. M. Berman, J. D. Bjorken, J. B. Kogut, *Phys. Rev.* **D4**, 3388 (1971); J. D. Bjorken, *Phys. Rev.* **D9**, 2027 (1974).
[10] S. D. Ellis, M. B. Kislinger, *Phys. Rev.* **D9**, 2027 (1974).
[11] J. Kripfganz, J. Ranft, CERN preprint CERN-TH 2244, 1976.
[12] V. Barger, R. J. N. Phillips, *Nucl. Phys.* **B73**, 269 (1974).
[13] R. D. Field, R. P. Feynman, Cal-Tech-preprint, CALT-68-565, 1976.
[14] G. R. Farrar, *Nucl. Phys.* **B17**, 429 (1974).
[15] R. McElhaney, S. F. Tuan, *Phys. Rev.* **D8**, 2267 (1973).
[16] B. L. Combridge, *Phys. Lett.* **62B**, 222 (1976).
[17] D. Sivers, S. Brodsky, R. Blankenbecler, *Phys. Rep.* **23**, 1 (1976).
[18] R. Raitio, Wisconsin University preprint COO 545, 1976.
[19] S. D. Ellis, M. Jacob, P. V. Landshoff, *Nucl. Phys.* **B108**, 93 (1976).
[20] K. Eggert et al., *Nucl. Phys.* **B18**, 49 (1975).
[21] D. C. Carey et al., *Phys. Rev. Lett.* **33**, 327 (1974).
[22] G. Ranft, J. Ranft, *Nucl. Phys.* **B110**, 493 (1976).
[23] G. Ranft, J. Ranft, Karl-Marx-University preprint KMU-HEP 76-14, Oct. 1976.